JETIR.ORG ISSN: 2349-5162 | ESTD Year : 2014 | Monthly Issue
JOURNAL OF EMERGING TECHNOLOGIES AND INNOVATIVE RESEARCH (JETIR)
An International Scholarly Open Access, Peer-reviewed, Refereed Journal

POWER QUALITY IN EVS WITH CASCADED MULTILEVEL INVERTER BY INTELLIGENT METHODS

[1]Ms. P SWATHI, [2]Mrs. A. ANURADHA

[1]PG scholar in the Dept. of Electrical & Electronics Engineering in Holy Mary Institute of Technology & Science, Bogaram (V), Medchal District, Hyderabad, India.

[2]Assistant Professor in the Dept. of Electrical & Electronics Engineering in Holy Mary Institute of Technology & Science, Bogaram (V), Medchal District, Hyderabad, India.

Abstract: ***Power transmission is a technique that uses power electronic circuits for communication signal transmission. In this paper, a three-phase cascaded multilevel inverter-based power transmission system is proposed. The proposed method can transmit communication signals without using a Controller Area Network bus, thereby reducing the wiring cost of the conventional electric vehicle (EV) communication system. The designed system can achieve motor speed regulation and battery balance discharging for EVs. This paper presents a Cascaded Multilevel Inverter with ANN (Artificial Neural Network) controller. The EV setup consists of a rectifier (AC/DC) in the front end and a converter (DC/DC) at the back end, with a DC link capacitor separating the converter and rectifier. The structure of the charger enables the capability of voltage control of the grid, due to its bidirectional flow of power. The effectiveness of ANN-based charger in grid voltage regulation in various modes of charging and discharging operations of Electric Vehicles (EV's).***

Index Terms—Battery state of charge, controller area network, frequency shift keying, motor speed control, pulse width modulation, three-phase DC-AC converter.

I. INTRODUCTION

The challenges posed by climate change are spurring experts and researchers to investigate the alternatives for fossil fuels to achieve carbon dioxide emissions reduction. Nowadays, the application of electric vehicles provides a feasible solution for energy saving and emission reduction in the automotive industry. Compared to the traditional internal combustion engine cars, electric vehicles (EVs) not only produce fewer air pollutants such as CO and NOx, but also generate less noise [1], [2]. Furthermore, if the battery of EV is charged at night, it can avoid the peak of power consumption, which is beneficial to the grid to balance the load and reduce the cost [3]. Since various subsystems such as the motor control unit (MCU) and the battery management system (BMS) in an EV require communication with the transmission control unit (TCU), it is necessary to employ an effective method to realize signals transmission [4], [5]. One of the approaches that is widely accepted by manufacturers and researchers for data transmission in EV is through a Controller Area Network (CAN) bus because of its high reliability and high communication baud rate [6], [7].

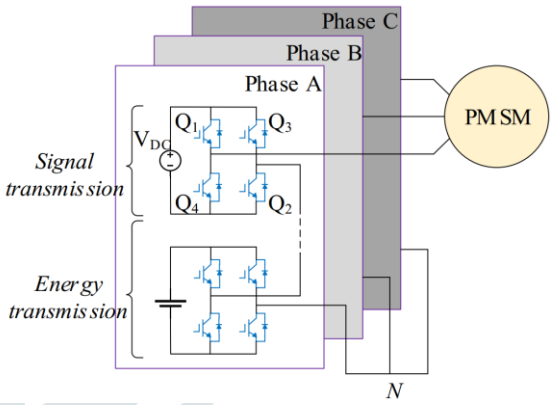

Fig. 1. The CBMLI of the proposed EV.

The general powertrain structure of an EV is exhibited in Fig.1. Some conventional power systems for EVs employ a DC/DC converter to boost the battery voltage for a 2-level inverter [8], [9]. This approach can have a high voltage change rates (dV/dt), which leads to high switching losses [8]. Moreover, such the system is expensive and has low power density because of the utilized bulky inductors for the DC/DC boost converters [9]. Although the traditional EVs realize their internal communication through the CAN bus, the communication channel and the power transmission line are still two independent sections, and the whole system can still be optimized.

This paper proposes a power & signal multiplex transmission (P&SMT) method to transmit both power and communication signals through a three-phase multilevel inverter circuit for EVs. The individual devices of the multilevel inverter have a much lower switching losses than that of a 2-level inverter, and a DC/DC converter is not required since the cascaded multilevel inverter itself can boost the battery voltage. In the proposed system, the power

conversion is realized by the pulse width modulation (PWM) method, and the transmitted signals are modulated by the frequency shift keying (FSK) approach. Instead of using a CAN bus as a communication channel in the up-to-date EVs, the proposed approach can greatly reduce the expenditure on the communication system because the power and signals are transmitted simultaneously through the same power line.

II. PROPOSED POWER AND SIGNAL MULTIPLEX TRANSMISSION

A. System Structure

This paper elaborates the principle of the proposed P&SMT method by using the transmitted battery state of charge (SOC) signal and motor speed control signal as an example. The proposed system structure of an EV using the P&SMT method is shown in Fig. 2. The communication between the battery and BMS, and that between the MCU and motor are realized by transmitting signals through a three-phase multilevel inverter circuit. The proposed topology of a three-phase P&SMT system is indicated in Fig. 3. Specifically, each phase of the inverter topology contains four series connected H-bridge cells, where the cell powered by a DC voltage source is used for signal transmission, and the rest three cells powered by batteries are applied for energy transmission. The motor speed adjustment signal and the SOC signal are transmitted through the phase A and phase B branch respectively. In this model, a permanent magnet synchronous motor (PMSM) is applied as a load of the inverter topology.

B. Signal Transmission

The signals are modulated by the FSK method in the proposed system and the signal transmission scheme is presented in Fig. 4. If the transmitted 4-bit signal SI is '1010', then two carriers with different frequencies shown in SC can be applied for modulating digital '1' and digital '0' respectively. Since the signal is designed to be transmitted through an H-bridge cell in each phase, such the signal can be modulated by controlling the fast switching process of the four switches in the cell. Specifically, a switch will turn on if a digital '1' is applied as a gate signal and it will turn off when digital '0' is used. In Fig. 3, the switches Q1 and Q2 operate simultaneously and the switches Q3 and Q4 turn on and turn off at the same time. Besides, the switches Q1 and Q2 operate with the opposite state to that of the switches Q3 and Q4 to avoid short circuit. Because the H-bridge cell used for signal transmission is series connected with the other three cells applied for energy transmission, the transmitted signal can be considered as superimposed on the output current waveform.

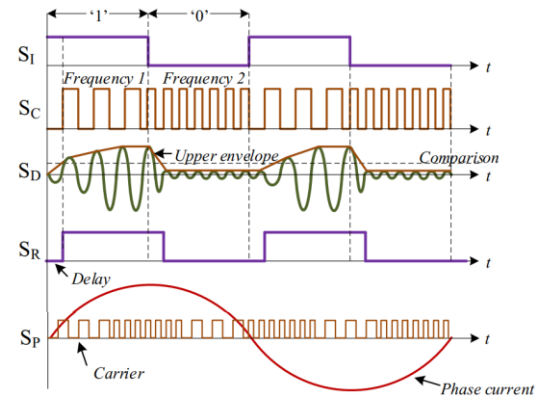

Fig. 2. The signal transmission scheme of the proposed system, where SI is the initial 4-bit signal '1010'; SC is the carrier waveform; SD represents the extracted carrier for digital '1' after using a band-pass filter; SR shows the restored signal; SP is the output phase current waveform superimposed with the signal's carrier.

Then a band-pass filter is employed to extract the transmitted signal from the output current waveform at receiver. For any signal f(x) with period T and angular frequency ω=2π/T, its Fourier series expansion can be expressed as

$$F(x)=\frac{1}{2}a_0+\sum_{n=1}^{\infty}\left(a_n\cos n\omega x+b_n\sin n\omega x\right)$$

where the coefficients and in this series are defined by

$$\begin{cases} a_0=\dfrac{2}{T}\displaystyle\int_{-T/2}^{T/2}f(x)\,dx \\ a_n=\dfrac{2}{T}\displaystyle\int_{-T/2}^{T/2}f(x)\cos n\omega x dx \\ b_n=\dfrac{2}{T}\displaystyle\int_{-T/2}^{T/2}f(x)\sin n\omega x dx \end{cases}$$

Similarly, if a square wave f(t) with period T is applied as a carrier for digital '1', it can be expressed as

$$f(t)=\begin{cases} 0 & -\dfrac{T}{2}\le t<0 \\ 1 & 0\le t\le\dfrac{T}{2} \end{cases}$$

The Fourier series expansion of f (t) is derived as

$$F(t)=\frac{1}{2}+\frac{2}{\pi}\sin x+\frac{2}{3\pi}\sin 3x+\frac{2}{5\pi}\sin 5x+\frac{2}{7\pi}\sin 7x+\ldots$$
$$+\frac{2}{n\pi}\sin nx$$

where n is an odd number. Because the Fourier series expansion of f(t) only contains the odd harmonic components, and the first-order harmonic has the largest amplitude, the first-order harmonic can be utilized for restoring the communication signals. For instance, the curve SD in Fig. 4 represents the demodulated carrier for digital '1', then its upper envelope can be acquired using an envelope detector. With an appropriate comparison value, the upper envelope can be recovered to digital '1' when its amplitude larger than the comparison value. Otherwise, it will be recovered to digital '0'. Finally, the restored SR is obtained after sampling the recovered digital signal using the initial bit rate of SI.

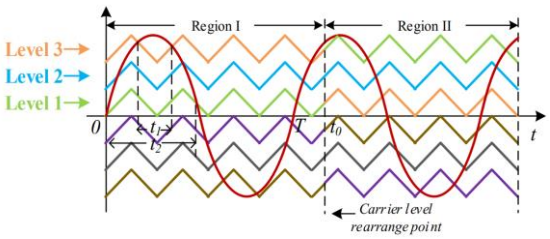

Fig. 3. Carrier level rearrangement in the PWM process.

C. Motor Speed Regulation and Battery Balance Discharging

In the proposed system, the motor speed is managed by setting the power frequency to different values with the transmitted signal. Expressly, the relationship among the motor speed n, pole-pair p, and power frequency f for a PMSM is indicated as

$$n = \frac{60f}{p}$$

where the constant 60 refers to 60 s/min. Theoretically, the speed of a 2-pole pair motor should change between 1200 r/min and 1800 r/min if its power frequency varies between 40 Hz and 60 Hz. With the transmitted signal s, the power frequency f is then calculated by

$$f = 20 \times s + 40$$

The power frequency will be 40 Hz and 60 Hz if the digital '0' and digital '1' occur in the transmitted signal s respectively. Next, the three-phase reference sinusoidal waves are obtained from where Pa, Pb, and Pc represent the reference wave in phase A, phase B, and phase C respectively, and A is amplitude. The phase B and phase C reference waves lag the phase A reference wave by 2π/3 and 4π/3 radians respectively. Finally, the modulated variable frequency sine waves are used to drive the motor to achieve motor speed adjustment.

$$\begin{cases} P_a = A\sin(2\pi f) \\ P_b = A\sin\left(2\pi f - \frac{2}{3}\pi\right) \\ P_c = A\sin\left(2\pi f - \frac{4}{3}\pi\right) \end{cases}$$

In the conventional sinusoidal PWM method, the gating signal of a switch is generated by comparing the reference wave with a triangular carrier. Because various carriers and the reference wave intersect at different positions, the duty cycle of each switch is different. For instance, in a single period from 0 to T as displayed in Fig. 5, the duty cycle of a switch controlled by 'Level 3' carrier is smaller than that of the other switch modulated by 'Level 1' carrier (t1<t2). Since the input power comes from batteries, the switch operating with a smaller duty cycle consumes less power than the switch operating with a larger duty cycle. This will further lead to the case of batteries' remaining capacity being unbalanced after the system running for a while. Therefore, the battery balance discharging can be realised by periodically rearranging the carrier levels within the PWM process. To achieve this target, firstly, the battery SOC values at the periodical sampling point are combined to form a data stream and transmitted through the DC voltage source powered full-bridge cell using FSK method. After demodulating the signal from the phase current, the SOC values are separated into different decimal numbers. Finally, the carrier levels of PWM are rearranged according to the transmitted SOC values (at t0 in Fig. 5 for example), and the battery balance discharging is realized.

III. ANN PERFORMANCE EVALUATION

ANN is a powerful tool for controlling a very complex in nature, nonlinear structure. Use a well-designed ANN to replace the look-up table and to produce optimal switching angles in real time [22]. A standard two-layer feed-forward network shown in Figure 5 with hidden sigmoid neurons and linear output neurons will arbitrarily fit well with multidimensional mapping problems. An input layer includes n inputs and vectors P, t1 sigmoid hidden neurons in the hidden layer and t2 linear output neurons in the output layer. Figure 5 demonstrates the ANN architecture including an input layer with two inputs, a hidden layer with two hidden neurons and a two-output output layer. A Simulink Model with delayed feedback loop is created using the ANN as shown in Figure 6.

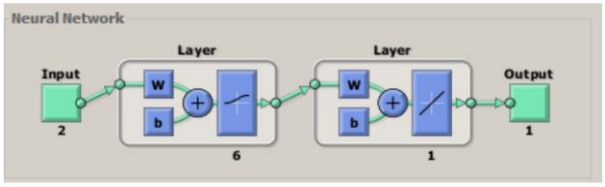

Figure 4. Simulink model for ANN-based neuron map chaotic system

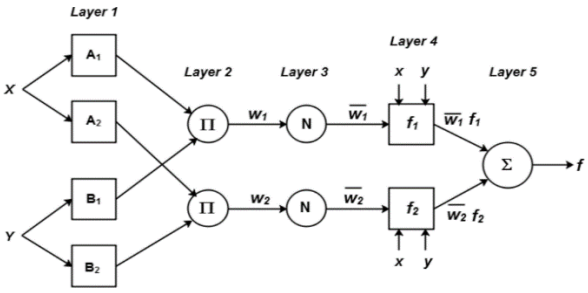

Figure 5. ANN controller block diagram

ANN controllers ' network structure is defined by the number of neurons in the respective input layer, hidden layer and output layer. To generate the proposed M-CHBMI switching signal, the first output layer neuron is used as the input to feed the PWM generator. The connections weight parameter between jth and ith neuron at mth layer is given by wmij, while bias parameter of this layer at ith neuron is given by bmi. Transfer function of the network at ith neuron in mth layer is defined by:

$$n_i^m = \sum_{j=1}^{S^{m-1}} W_{ij}^m a_j^{m-1} + b_i^m$$

Neurons output function at the m[th] layer is given by

$$a_i^m = f^m(n_i^m)$$

Where f is neuron activation function. The activation function of the output layer is unity in this design and a tangent hyperbolic function for the hidden layer is given by

$$f^m(n_i^m) = \frac{2}{1+e^{-2n_i^m}} - 1$$

IV. SIMULATION RESULTS AND ANALYSIS

Simulation Parameters and Output Waveforms

Based on the mechanisms demonstrated, a simulation model is built in Matlab/Simulink. Table I summarises the values of parameters in the simulation model. Each H-bridge cell for power transmission contains a 48 V battery, and a 30 V DC voltage source is applied in each H-bridge circuit for signal transmission. Therefore, the amplitude of the transmitted signal is neither too small to be restored, nor too large to seriously affect the output sinusoidal waveform. Moreover, because the system employs the carriers with the frequency distribution from 2 kHz to 10 kHz, it is appropriate for silicon type IGBT devices to operate in such a frequency range [20]. When connecting a PMSM as a load to the output side of the three-phase inverter circuit, the output voltage and current waveforms measured by a voltage sensor and a current sensor are exhibited in Fig. 2. Since there are three batteries and a DC voltage source in each phase, the maximum phase voltage is 174 V (3×48+30=174). It can be observed that the amplitude of the phase current waveform varies at around 0.27 s and 0.51 s, and this is because the motor power frequency changes from 40 Hz to 60 Hz at these time points.

TABLE I

PARAMETERS VALUE USED IN THE PROPOSED SYSTEM

Parameter name	Value
DC voltage source	30 V
Battery voltage	48 V
PWM carrier frequency	2 kHz
PWM referenced sine wave frequency	40 Hz, 60 Hz
Carrier frequency of motor speed adjustment signal	4 kHz for '1' and 8 kHz for '0'
Carrier frequency of SOC signal	6 kHz for '1' and 10 kHz for '0'

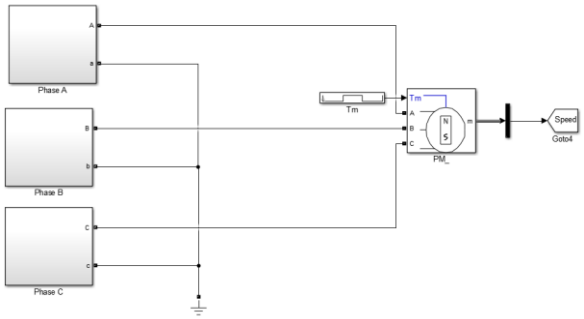

Fig 6. Simulation diagram of the proposed system.

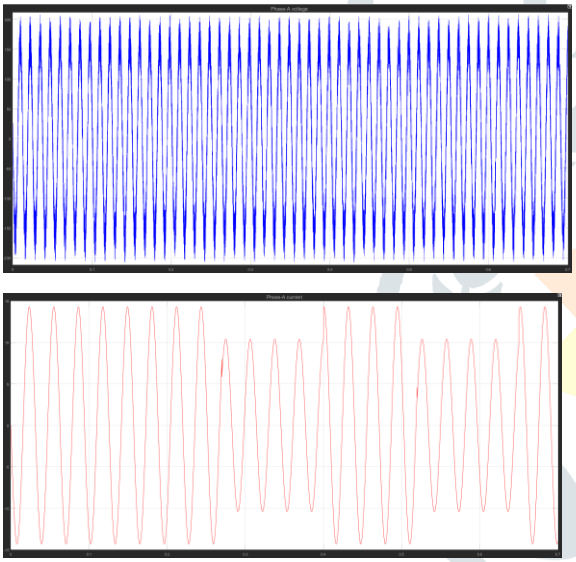

Fig. 7. (a) The output voltage waveform of phase A and (b) the output current waveform of phase A.

Motor Speed Adjustment Signal Transmission

An original 8-bit motor speed adjustment signal is set as 11110000 with 0.03 s per bit, thus the signal transmitting rate is 100/3 bps. Then a 4-bit cyclic redundancy code (CRC) is added at the end of each 8-bit data string to separate two adjacent data strings. Because the generated 4-bit CRC code is 0100 by using the generator polynomial , the entire 12-bit data frame is 111100000100. Dividing the transmitted data frame by the modulo-2 division approach with the divisor 11110, the system can determine whether the frame data is erroneous by verifying whether the remainder is zero. If it is 0, it proves that the frame data has no errors during the transmission, otherwise an error occurs. Both the original message data and the message data followed by the CRC code is shown in Fig. 3. It is worth mentioning that the time used for transmitting a frame with a CRC code and without a CRC code are the same, thus the 12-bit data is transmitted with 0.02 s per bit. After the entire data frame is obtained, the 4 kHz square wave is applied as a carrier for digital '1' and the 8 kHz square wave is used as a carrier for digital '0'. Next, the signal is transmitted through an H-bridge cell, and the 4 kHz carrier is extracted from the phase current waveform with a band-pass filter. Then the filtered carrier waveform SF in Fig. 8 is used to recover the transmitted signal with an appropriate threshold value. Since the attenuation at cut-off frequencies is fixed at 6 dB in this band-pass filter, the attenuation ratio x can be calculated as 0.5 from

$$20\log x = -6$$

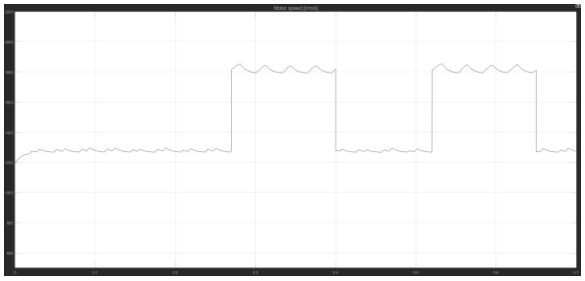

Fig. 8. The controlled motor speed with the transmitted 8-bit signal '11110000'.

In other words, the amplitude of waveform SF in cut-off frequencies region (0.04) is half of its amplitude in the passband frequencies region (0.08). Therefore, '0.05' is selected to separate the cut-off frequencies region and passband frequencies region of the filtered wave. When collating the recovered signal SST in Fig. 4 with the waveform SE in Fig. 3, it can be observed that there exists a delay in SST, which is mainly caused by the filtering process. After removing the 4-bit CRC code after each 8-bit data frame, the restored signal SRE in Fig. 4 is obtained. Because the 4-bit CRC code first occurs at 0.18 s (0.02×8+0.02(one-bit delay)=0.18), the transmitted data before the CRC code in the first period is 'ignored' by the system. Additionally, the recovered data frame has the same rate (0.03 s per bit) as its original signal rate. Therefore, the restored 8-bit data frame first appears at 0.27 s (0.03×8+0.03(one-bit delay)=0.27), and SRE can be considered as delaying a whole signal period plus one sampling time.

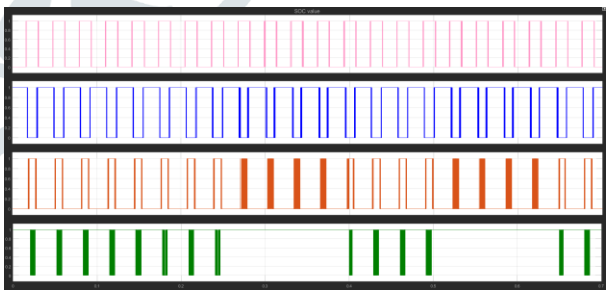

Fig. 9. SCB is the code string formed by the three SOC frames; SRB is the recovered SOC signal; SBA1 contains the frame '01100100', which indicates the SOC of the first battery; the frame '00101000' in SBA2 refers to the SOC of the second battery; the frame '00100011' in SBA3 represents the SOC of the third battery.

Finally, the recovered signal SRE in Fig. 5 is utilized to manage the motor speed, whose waveform is displayed in Fig. 6. Whenever the signal changes between '0' and '1', the motor speed fluctuates for about 0.01 s. Since the power frequency is designed to alternate between 40 Hz and 60 Hz, the motor speed stabilizes at 1200 r/min and 1800 r/min as expected. Because the transmitted signal is superposed on the phase current in the form of energy, the transmitted signal will interfere with the phase current waveform, thus affecting

the stability of motor speed. Additionally, as the motor speed is open-loop controlled by adjusting the motor power frequency, its steady-state fluctuation is larger than the conventional double closed-loop control approach.

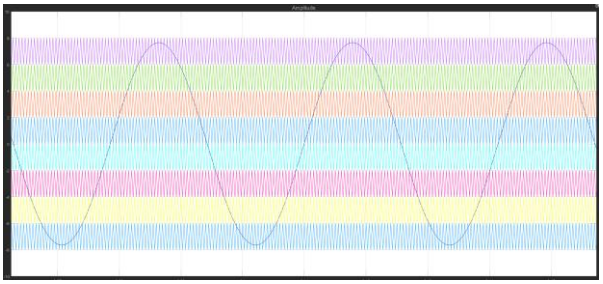

Fig. 10. The rearranged carriers and the reference sinusoidal wave used in the PWM process, where (a) is the original image, and (b) is the enlarged image at the carrier level rearrange point.

System Data Transmission Capability

The maximum data transmission rate of the proposed system can be determined by calculating the error rate of the transmitted signal. When comparing the original data string and the received one bit by bit, the error rate of the transmitted signal is obtained. After gradually increasing the rate of the motor speed control signal, the relationship between the bit rate and the error rate is exhibited. From this figure, the error rate starts rising when the signal rate is larger than 600 bit/s. Since the proposed system manages the batteries' discharge process according to the batteries' SOC value, there is an extremely high requirement for the correctness of the transmitted data. Once the demodulated data is incorrect, the batteries SOC sequencing does not achieve the expected results. The data rate of this system is relatively low when comparing to the conventional communication channels such as optical fibre. However, such a low data rate is acceptable in this system as the batteries' SOC value does not change significantly in a short time. Moreover, because the motor speed takes a while to stabilize after the frequency changes at each time, it is sufficient to transmit the motor speed control signal at a data rate of 600 bit/s.

CONCLUSION

In this paper, a three-phase multilevel inverter-based P&SMT system is proposed to achieve motor speed adjustment and battery balance discharging for EVs. Four series-connected H-bridge cells are involved in each phase of the inverter topology, where the PWM controlled three cells are used for energy transmission and the rest FSK controlled cell is applied for communication signal transmission. However, due to the switching angles of the ANN technique, the ANN technique produces lower THD content of the modified CHB-MLIs output voltage waveform compared with the ANN technique. "However, the ANN technique produces a lower THD content of the modified CHB-MLI output voltage and current waveform, because the switching angles of the ANN technique are simple and efficient. With a simulation model implemented in Matlab/Simulink, the feasibility of the proposed P&SMT method is verified by transmitting the motor speed adjustment signal and the battery SOC signal through phase-A and phase-B currents respectively.

REFERENCES

[1] T. Donateo, F. Licci, A. D'Elia, G. Colangelo, D. Laforgia and F. Ciancarelli, "Evaluation of emissions of CO2 and air pollutants from electric vehicles in italian cities," Applied Energy, vol. 157, pp. 675-687, Nov. 2015.

[2] C. Ma, C. Chen, Q. Liu, H. Gao, Q. Li, H. Gao and Y. Shen, "Sound quality evaluation of the interior noise of pure electric vehicle based on neural network model," IEEE Transactions on Industrial Electronics, vol. 64, no. 12, pp. 9442-9450, 2017.

[3] M. Yilmaz and P. T. Krein, "Review of the impact of vehicle-to-grid technologies on distribution systems and utility interfaces," IEEE Transactions on Power Electronics, vol. 28, no. 12, pp. 5673-5689, 2013.

[4] K.Ç. Bayindir, M.A. Gözüküçük and A. Teke, "A comprehensive overview of hybrid electric vehicle: Powertrain configurations, powertrain control techniques and electronic control units," Energy conversion and Management, vol. 52, no. 2, pp. 1305-1313, 2011.

[5] X. Zhu, H. Zhang, J. Xi, J. Wang and Z. Fang, "Optimal speed synchronization control for clutchless AMT systems in electric vehicles with preview actions," 2014 American Control Conference, pp. 4611-4616, 2014.

[6] F. Zhou, S. Li and X. Hou, "Development method of simulation and test system for vehicle body CAN bus based on CANoe," 2008 7th World Congress on Intelligent Control and Automation, pp. 7515-7519, 2008.

[7] M. Zheng, B. Qi and H. Wu, "A li-ion battery management system based on CAN-bus for electric vehicle," 2008 3rd IEEE Conference on Industrial Electronics and Applications, pp. 1180-1184, 2008.

[8] L. M. Tolbert, F. Z. Peng and T. G. Habetler, "Multilevel inverters for electric vehicle applications," Power Electronics in Transportation (Cat. No.98TH8349), pp. 79-84, 1998.

[9] Z. Du, B. Ozpineci, L. M. Tolbert and J. N. Chiasson, "DC–AC cascaded H-bridge multilevel boost inverter with no inductors for Electric/Hybrid electric vehicle applications," IEEE Transactions on Industry Applications, vol. 45, no. 3, pp. 963-970, 2009.

[10] L. Lampe, A.M. Tonello and T.G. Swart, Power Line Communications: Principles, Standards and Applications from multimedia to smart grid, John Wiley & Sons, 2016.

[11] W. Huagang, T. R. Meng and L. S. Wen, "Measurement and analysis of electromagnetic emissions for broadband power line (BPL) communication," 2017 IEEE 5th International Symposium on Electromagnetic Compatibility (EMC-Beijing), pp. 1-4, 2017.

[12] R. V. White, "Electrical isolation requirements in power-over-ethernet (PoE) power sourcing equipment (PSE)," Twenty-First Annual IEEE Applied Power Electronics Conference and Exposition, 2006. APEC '06, pp. 4, 2006.

[13] J. Herbold, "Navigating the IEEE 802.3af standard for PoE," POWER ELECTRONICS TECHNOLOGY, vol.30, no. 6, pp. 45-48, 2004.

[14] W. Xu and W. Wang, "Power electronic signaling Technology—A new class of power electronics applications," IEEE Transactions on Smart Grid, vol. 1, no. 3, pp. 332-339, 2010.

[15] S. Saggini, W. Stefanutti, P. Mattavelli, G. Garcea and M. Ghioni, "Power line communication in dc-dc converters using switching frequency modulation," Twenty-First Annual IEEE Applied Power Electronics Conference and Exposition, 2006. APEC '06, 2006.

[16] W. Stefanutti, P. Mattavelli, S. Saggini and L. Panseri, "Communication on power lines using frequency and duty-cycle modulation in digitally controlled dc-dc converters," IECON 2006 - 32nd Annual Conference on IEEE Industrial Electronics, pp. 2144-2149, 2006.

[17] W. Stefanutti, S. Saggini, P. Mattavelli and M. Ghioni, "Power line communication in digitally controlled DC–DC converters using switching frequency modulation,"IEEE Transactions on Industrial Electronics, vol. 55, no. 4, pp. 1509-1518, 2008.

[18] J. Wu, C. Li and X. He, "A novel power line communication technique based on power electronics circuit topology," 2010 Twenty-Fifth Annual IEEE Applied Power Electronics Conference and Exposition (APEC), pp. 681-685, 2010.

[19] J. Wu, S. Zong and X. He, "Power/signal time division multiplexing technique based on power electronic circuits," 2011 Twenty-Sixth Annual IEEE Applied Power Electronics Conference and Exposition (APEC), pp. 1710-1714, 2011.

[20] C. Blake and C. Bull, "IGBT or MOSFET: Choose wisely," International Rectifier, 2001.

AUTHORS DETAILS

Mrs. A. Anuradha received a B. TECH degree in EEE from Christu Jyothi Institute of Technology and cience, Colombo Nagar, Yeshwanthpur, Jangaon, Telangana, from JNTUH University and an M.TECH in power systems at Vignana Bharathi Institute of Technology, Aushapur, Ghatkesar, Near HPCL, Hyderabad, Telangana, India. Currently working as Assistant professor in Holy Mary Institute of Technology and science, Bogaram, Medchal District, Hyderabad, Telangana, India in the EEE department.

Ms. P Swathi received a diploma in electrical and engineering from Government Polytechnic College, Mahabubnagar Telangana, India, and received a B.Tech degree in EEE from Gokaraju Rangaraju institute of engineering and technology, Bhachupally, Kukatpally, Hyderabad, Telangana, India from JNTUH University .and studying in M.Tech in Electrical Power Systems at Holy Mary Institute of Technology and Science, Bogaram (vi), Medchal (di), Hyderabad, Telangana, India, in the department of electrical and electronics engineering.